JOURNAL OF GEOPHYSICAL RESEARCH, VOL. ???, XXXX, DOI:10.1029/,

Impact of global seismicity on sea level change assessment

D. Melini and A. Piersanti

Istituto Nazionale di Geofisica e Vulcanologia, Rome, Italy

D. Melini, Istituto Nazionale di Geofisica e Vulcanologia, Via di Vigna Murata 605, I-00143 Roma, Italy. (melini@ingv.it)

Abstract. We analyze the effect of seismic activity on sealevel variations, by computing the time-dependent vertical crustal movement and geoid change due to coseismic deformations and postseismic relaxation effects. Seismic activity can affect both the absolute sealevel, by changing the Earth gravity field and hence the geoid height, and the relative sealevel, i.e. the radial distance between seafloor and geoid level. By using comprehensive seismic catalogues we assess the net effect of seismicity on tidal relative sealevel measurements as well as on the global oceanic surfaces, and we obtain an estimate of absolute sealevel variations of seismic origin.

We improved the computational methods adopted in previous analyses considering the issue of water volume conservation through the application of the sealevel equation and enabling us to evaluate the effect of an extremely large number of earthquakes on large grids covering the whole oceanic surfaces. These new potentialities allow us to perform more detailed investigations discovering a quantitative explanation for the overall tendency of earthquakes to produce a positive global relative sealevel variation. Our results confirm the finding of a previous analysis that, on a global scale, most of the signal is associated with few giant thrust events, and that RSL estimates obtained using tide-gauge data can be sensibly affected by the seismic driven sealevel signal.

The recent measures of sealevel obtained by satellite altimetry show a wide regional variation of sealevel trends over the oceanic surfaces, with the largest deviations from the mean trend occurring in tectonically active regions. While

our estimates of average absolute sealevel variations turn out to be orders of magnitude smaller than the satellite measured variations, we can still argue that mass redistribution associated with aseismic tectonic processes may contribute to the observed regional variability of sealevel variations. A detailed study of these tectonic contributions is important to acquire a complete understanding of the global sealevel variations and will be subject of future investigations.

1. Introduction

Current estimates of relative sealevel variations on a secular time-scale based on tide-gauge measurements indicate a uniform rise in the range 1.75 ± 0.55 mm/yr [*Douglas et al.*, 2001; *White et al.*, 2005]. The uncertainty on this figure depends on the particular subset of observations employed, on their scatter, and on the method used to correct the data for vertical land movements due to glacial isostatic adjustment (GIA) [*Mitrovica and Davis*, 1995]. The main contributions to last decades sealevel rise come from thermal expansion of oceans due to global warming and ocean mass change due to glaciers and ice sheet melting.

Recent observations from satellite altimetry [*Cazenave and Nerem*, 2004] over the decade 1993–2003 gave a larger rate (3.1 mm/yr after removing GIA effects) and, by allowing for measurements of sealevel on the whole oceanic surfaces, evidenced a strong nonuniform geographical distribution of sealevel changes, with some regions exhibiting rates about 10 times greater than the global mean and some other regions where the trend was inverted and negative variations up to 15 mm/yr were detected.

Since seismic events alter the equilibrium state of the solid Earth and perturbate its gravitational field, they are also likely to produce sealevel variations. The perturbation of the Earth's gravity field due to mass redistribution following a seismic event affects the geoid level and it is therefore responsible for a variation in the absolute sealevel. The vertical deformation of the seafloor, together with the geoid change, produce also a relative sealevel change. Relative sealevel is directly measured at tide-gauge stations, while absolute sealevel is measured by satellite altimetric missions.

In a previous work [*Melini et al.*, 2004], we investigated the effect of global seismic activity on the observed relative sealevel variations, and found that great earthquakes have an overall tendency to produce a sealevel rise, affecting the measurements taken at those tide-gauge sites commonly employed for sealevel rise monitoring. On a global scale, most of the signal is associated with few giant thrust events that, depending on the viscosity of the asthenosphere, can induce a sealevel signal of at least 0.1 mm/yr. This result has been obtained adopting the seismic catalogue considered by *Marzocchi et al.* [2002], which contains 778 shallow earthquakes (depth $\leq$ 70km) with magnitude $M \geq 7$, and includes events from the *Pacheco and Sykes* [1992] compilation and the CMT catalogue [*Dziewonski et al.*, 1981].

Estimates of sealevel rise coming from water volume increase due to ocean warming give a rate of about 0.5 mm/yr while the rate due to mass increase from ice melting is highly controversial and recent estimates range from less than 0.5 mm/yr to 1.5 mm/yr [*Levitus et al.*, 2000; *Miller and Douglas*, 2004]. Therefore, the average contribution to RSL coming from seismic activity maybe comparable with estimates of individual climatological factors and, in regions with strong seismotectonical activity, may represent locally a major contribution to RSL.

In this work, we compute the seismic contribution to sealevel rise on the whole oceanic surfaces with a self-consistent approach that takes into account ocean volume conservation. We use as seismic datasets both the catalogue considered by *Marzocchi et al.* [2002] and the CMT catalogue up to July 31, 2004. The seismic dataset by *Marzocchi et al.* [2002] covers a longer time window, which is a crucial feature in assessing long-term effects, while the CMT catalogue has a shorter temporal coverage but it is characterized by a

lower magnitude threshold and provides more reliable estimates of focal parameters. We find that the global mean of sealevel trends induced by earthquakes is positive, but its geographical distribution is higly variable, with a pattern that shows several analogies with the satellite measurements [*Nerem and Mitchum*, 2002; *Cazenave and Nerem*, 2004].

We also quantified the effect of CMT seismic activity on tide-gauge measurements as we did in *Melini et al.* [2004] for the *Marzocchi et al.* [2002] catalogue. While the CMT results qualitatively confirm the ones obtained previously, their absolute value is much smaller, most likely because of the absence of giant subduction events like Chile 1960 and Alaska 1964 in the CMT catalogue.

On December 26, 2004, an exceptionally large event stroke the Indonesian region. According to current estimates, it is probably the second largest event ever registered. We present here some preliminary result about its effect on sealevel.

In order to gain better insight into the reasons for the global tendence of seismicity to produce positive sealevel variations, we performed a detailed synthetic analysis, investigating separately the contributions to vertical displacements and geoid variations. We also computed separately the RSL field induced by 1960 Chile and 1964 Alaska earthquakes and found that these two earthquakes alone account for a large fraction of the seismically-driven sealevel signal. Beyond this, we found that the reciprocal geometrical features of the relative sealevel signal associated with these two events and the distributions of the tide gauge stations is mostly responsible for the positive mean in the computed relative sealevel trend.

2. Method

2.1. Postseismic deformation modeling

To compute the time-dependent deformation and gravity field variations associated with a seismic dislocation we adopted the model proposed by *Piersanti et al.* [1995], a spherical model which assumes an incompressible, layered, self-gravitating Earth with Maxwell linear viscoelastic rheology. The model was later refined by *Soldati et al.* [1998] to account for gravitational effects and by *Boschi et al.* [2000] to include the contribution of deep (upper mantle) earthquakes. We refer the reader to these works for details concerning the numerical approach.

We employed a 4-layer stratification which includes an 80 km elastic lithosphere, a 200 km thick low-viscosity asthenosphere with $\eta = 10^{19}$ Pa s, appropriate for oceanic asthenosphere [*Cadek and Fleitout*, 2003], a uniform mantle with $\eta = 10^{21}$ Pa s and a fluid inviscid core. All the other mechanical parameters have been obtained by means of a weighted volume average of the corresponding parameters of PREM model.

Of course, our results depend on the chosen viscosity values. The effect of varying asthenosphere and mantle viscosity on the evolution of geophysical observables in the postseismic relaxation process has been extensively discussed in a series of works [*Piersanti et al.*, 1995, 1997; *Soldati et al.*, 1998; *Boschi et al.*, 2000; *Nostro et al.*, 2001] to which we refer the reader for more details. Roughly, we can say that viscosity values smaller than those employed here would further enhance the postseismic contribution to deformation and gravity fields, while the purely elastic coseismic response would remain unchanged.

With this model, we computed the time-dependent deformation and gravity field variations due to each seismic event in our catalogues. The time-dependent relative sealevel

$S(t)$ at a given observation site is then computed from the vertical displacement u_z and geoid variation G as $S(t) = G(t) - u_z(t)$.

The procedure to retrieve the numerical solution from our model involves a spherical harmonic expansion of the physical observables. Since the convergence of the harmonic series is very slow, it is needed to sum up to very high harmonic degrees ($1000 \leq l \leq 8000$, depending on source parameters), which requires huge computational resources. Since we had to evaluate the contribution of over 20,000 earthquakes, we implemented our codes on a parallel distributed-memory computer based on 48 Intel Xeon CPUs, where the whole simulation procedure required about 2 months of CPU time to run.

2.2. Conservation of water volume

The modeling approach described above allows us to estimate the sea level variation from the local changes in geoid height and seafloor vertical displacements. However, when dealing with global modeling, we should consider the problem of conservation of total water mass. The most general approach to the problem of ocean water conservation is expressed by the "sea level equation" (SLE), which takes into account the contribution of geoid changes and vertical seafloor displacements over the whole ocean [*Douglas et al.*, 2001; *Peltier*, 1998]. Moreover, SLE includes the immission of freshwater from melting of continental ice sheets (which are a major factor in postglacial sealevel variations) as well as the variation of the ocean function.

In the present approach, the conservation of total water mass is a direct consequence of our formulation, since we do not admit any water mass exchange; also, we don't include the effect of global warming, so we can assume constant water density; from these assumptions follows the conservation of total water volume. Consequently, instead of using the most

general form of SLE, we can use a simplified approach. Let $u_r(\theta, \phi, t)$ and $G(\theta, \phi, t)$ be the vertical seafloor displacement and geoid change at coordinates (θ, ϕ) and time t. We can express the total water volume conservation as:

$$\int_{\Omega'} \left(G(\theta, \phi, t) - u_r(\theta, \phi, t)\right) r_T^2 d\Omega = 0 \tag{1}$$

where r_T is the Earth radius and the integration is carried out over the surface of the oceans. Since we are dealing with very small sealevel variations, we can safely neglect the variations of the ocean function and assume the integration domain Ω' to be constant.

In our modeling approach the conservation of water volume is not automatically guaranteed, so we have to correct our computations to assure the validity of equation 1. To this aim, if G_0 is the geoid change associated with seismic activity, we can introduce a correction G_1 so that the total geoid variation $G = G_0 + G_1$ satisfies equation 1. Since we are dealing with small sealevel variations, at first order we can assume that this offset is constant over the oceanic surface, so that from equation 1 follows

$$G_1(t) = -\frac{\int_{\Omega'} \left(G_0(\theta, \phi, t) - u_r(\theta, \phi, t)\right) r_T^2 d\Omega}{\int_{\Omega'} r_T^2 d\Omega} \tag{2}$$

and we can write the relative sealevel at a given observation site as $S(t) = G_0(t) - u_r(t) + G_1(t)$.

The computation of the correction term in eq. 2 involves the numerical integration of $G_0(\theta, \phi, t)$ and $u_r(\theta, \phi, t)$ over the oceanic surface. Since the deformation field of earthquakes has very strong spatial variations in the near field, to carry out the numerical integration a dense sampling of the integrand function is required. The point dislocation approximation that we used in our simulations represents a further potential error source in the evaluation of the integral, because it produces large, unrealistic values of the fields

near the source. Beyond this, Since we are dealing with simulations involving over 20,000 seismic events, we found that, even adopting a massive parallel computing approach, in order to keep the simulation time acceptable (of the order of one month of CPU time) we cannot perform the integration of eq. 2 for the whole seismic dataset. We considered instead a set of 8 extremely large earthquakes occurred in the Pacific area, which account for about 80% of the total seiemic moment release in the last century [*Casarotti et al.*, 2001]. Since most of the seismic sealevel variation signal is associated with the largest events, we computed the cumulative $G_1(t)$ with these 8 events and used it to correct the sealevel time histories computed with the rest of the seismic dataset.

To assess the effect of point source approximation in the near-field geoid changes, we integrated eq. 2 both using the whole integration domain and excluding grid points located within a cutoff distance d from the seismic source. In figure 1 we compare the time-dependent $G_1(t)$ computed without cutoff and with $d = 50, 100, 200$ km. From this figure we can infer that the correction due to water volume conservation is strongly dependent on the chosen cutoff value, confirming that near-field effects give large contributions to G_1. Since the application of an integration cutoff strongly affects the final correction term and can shadow the physical signal, we decided to use the correction without cutoff to avoid the introduction of any arbitrary (operator dependent) bias. We emphasize that this correction is strongly dependent by the near-field signal, where we get ureliable values of dislocation and gravity fields because of the point source representation, and therefore G_1 will be undoubtly affected by approximation errors which may be quite large.

2.3. Seismic datasets

To compute the sealevel changes due to cumulative global seismicity we adopted two different catalogues. The first is the one considered by *Marzocchi et al.* [2002], and includes 778 shallow (depth ≤ 70 km) magnitude M ≥ 7 earthquakes worldwide distributed in the period $1900-1999$. This dataset was compiled including data from the Centroid Moment Tensor (CMT) [*Dziewonski et al.*, 1981] and *Pacheco and Sykes* [1992] catalogues; the focal parameters of the events taken from the Pacheco and Sykes catalogue have been estimated by using the moment tensor of the neighbor earthquakes reported by the CMT catalogue occurred within a certain distance from the Pacheco and Sykes epicenter, as explained by *Marzocchi et al.* [2002]. From now on, we will refer to this catalogue as "PS".

The second catalogue is the whole CMT catalogue, from January 1, 1976 up to July 31, 2004 that contains 21,708 events with magnitude M ≥ 4.7.

Basically, the PS catalogue covers a longer time window and includes the greatest events of the last century while the CMT catalog contains much more earthquakes with more reliable focal parameters, but it is characterized in average by much less energetic events. As a consequence, we could roughly say that the CMT catalog gives more precise information on the small scale features of the temporal evolution of RSL signal at each site while the PS catalog give more realistic results about the absolute magnitude of the seismic driven RSL signal.

3. Results

In our previous investigations [*Melini et al.*, 2004], we computed sealevel variations of seismic origin only at the sites of PSMSL tide-gauge stations, also because the solution

of the numerical model on a large number of points, such as a grid spanning the oceanic surfaces, had too heavy computational requests. For this work, we developed a further optimized version of the numerical code exploiting a massive parallelism, that enables us to compute the relative sealevel variations on the whole oceanic surfaces and to use, at the same time, a much larger number of seismic sources, such as the ones reported by the CMT catalogue.

3.1. Global effects

Figures 2 and 3 show the magnitude of relative sea level variations, in the whole oceanic surface, computed at different time steps, due to the net effect of all the earthquakes contained in the PS and CMT catalogues, respectively.

The results obtained with PS catalogue, shown in figure 2, have been corrected to account for the conservation of total water volume as described in section 2.2. Since the greatest earthquakes of the last century used to compute the geoid correction are included only in the PS catalogue, we didn't apply it to the results obtained with the CMT catalogue.

Even from a quick look at figures 2 and 3 we can see that the net effect of seismicity is a global increase of sealevel and that the magnitude of the induced variations shows a highly spatial variability reaching in some regions values of several centimeters. We see also that nearly all the coastlines are located within zones of positive RSL variation, while the larger areas of negative RSL variation are mostly placed far from the coasts. Since the vast majority of PSMSL tide-gauge stations are located along the coastlines, we expect that when we compute the effect of seismically-driven RSL on the PSMSL station sites

we will find a positive signal, as, in fact, we did in our previous analyses [*Melini et al.*, 2004].

By comparing figures 2 and 3 we can see also that the RSL effect of earthquakes contained in the CMT catalog, which lacks the giant thrust events of the last century, turns out to be at least one order of magnitude smaller than the effect of PS seismicity. In fact, when we look at the temporal variation of sealevels in figure 2, the largest contribution to sealevel variations almost on the whole oceanic surface comes in the interval (1960–1970), where we register the occurrence of the 1960 Chile and 1964 Alaska earthquakes. This is a confirmation of what we obtained when looking at the seismic RSL effects on the time-histories of tide-gauge measurements [*Melini et al.*, 2004], i.e. that earthquake–induced sealevel variations are mainly due to the effect of a few big earthquakes rather than the superposition of many small contributions.

The recent launch of altimetric satellite missions allowed to obtain independent estimates of sealevel variations. The TOPEX/Poseidon mission [*Nerem*, 1995, 1997] measured absolute geocentric sealevels along a ground track uniformly covering the oceanic surfaces. The acquired dataset covers the last decade (1993–2003) and indicates a mean sealevel rise of 3.1 mm/yr after correcting for GIA [*Cazenave and Nerem*, 2004].

In the same time window, our results give a global mean of order 10^{-3} mm/yr for relative sealevel while the rate for absolute (i.e. geoid) changes are an order of magnitude smaller. The sealevel trends obtained by global measurements such the ones carried out by TOPEX/Poseidon are, in fact, mainly due to thermal expansion of ocean water in response to global warming. Though it is clear that the global seismic selalevel signal is by far too small to be compared with the total detected signal nevertheless it represents only a facet

of the broader problem of global tectonic effects on sealevel. In this respect, it is reasonable to consider that the RSL signal associated with seismic events is higly correlated, and probably much smaller, with that associated with the whole tectonic processes since they share a common physical origin. Therefore, even if a direct comparison between seismic driven sealevel variations and measured trends is not possible, we remark that the role played by the whole tectonic processes could be important. Also the fact that in the detected data the main deviations from the mean sealevel trend are located in tectonically active regions, suggests that this topic deserves further investigations.

3.2. Effects on PSMSL sites

In figure 4 we show the rate of earthquake-induced relative sealevel variations expected at each of the 1016 PSMSL tide–gauge stations due to the cumulative effect of the CMT catalogue seismicity. The plotted values have been computed by least-squares interpolation of the time-series $S(t)$ over (1976-2003); red and blue circles indicate sealevel rises and falls, respectively. In figure 5 we plot the separate contribution to RSL variations due to near-field sources (distance from the tide-gauge within 500 km) and far-field sources (distance is greater than 500 km).

Also from the results of figure 4 we obtain that the effect of seismicity on the RSL variations measured by tide-gauge stations is a positive trend. According to our simulations, the average rate $\sum_k S_k/N$ over all the 1016 PSMSL sites is 0.019 mm/yr for the CMT catalogue (while for the PS catalogue we found 0.25 mm/yr). Major deviations from the general trend are observed in the Mediterranean area and along the circumpacific ring (North American west coast, Chile and Peru).

When we look at the RSL fields of figures 2 and 3 we can see that the areas where we obtain a negative variation are limited in extension, except for the large negative lobe off the Pacific coast of South America, that is associated with the 1960 Chile event. This behavior suggests that the negative sealevel variations are generally associated with the local effect of relatively small events. Indeed, when we separate the contributions to RSL measured by tide-gauges coming from "near" and "far" earthquakes (figure 5), we see that most of the negative contributions comes from earthquakes located within 500 km from the tide-gauge.

In figures 6 and 7 we turn our attention to the details of sealevel time-histories of the same PSMSL tide-gauge stations which have been considered by *Douglas* [1997] for his estimate of long-term sealevel rise. This set of 24 sites have been selected by Douglas for the length of sealevel records, which exceeds 70 years, for their expected tectonical stability and for their worldwide coverage. We have grouped these PSMSL sites regionally as done by *Douglas* [1991, 1997].

When we look at the effect of PS seismicity (figure 6) we can see that most of the seismic RSL signal is due to the coseismic effects of a few giant earthquakes, mainly the 1960 Chile and 1964 Alaska earthquake. The postseismic relaxation plays an important but not primary role, except for the stations located near the epicenter of large events (i.e. San Francisco, Quequen, Buenos Aires). However, in these cases the point source approximation used in our analysis gives unreliable results and a more realistic computation, based on a finite size seismic source, is needed. On the other hand, in the RSL time–histories obtained from CMT seismicity (figure 7) we see that the dominant effect comes from postseismic relaxation, because of the absence of giant earthquakes in the time

window covered by the catalogue. This figure allows us also to evaluate the impact of the correction for water volume conservation on the total RSL signal; though not negligible, we can see that its effect becomes important only in those sites where modest values of seismic RSL signal are registered.

In figure 8 we compared the RSL time–histories obtained using PS and CMT catalogues in the period 1976-2000, where the two datasets overlap. The time–histories obtained with the two seismic catalogues show a correspondence of the coseismic step-like signals produced by large earthquakes. Since the CMT catalogue includes much more events, because of its lower magnitude threshold, in some cases it may happen that a $M_w < 7$ event (i.e. not included in PS) located near a tide-gauge station gives a strong signal in the CMT time-history which is not found in the PS catalogue. This is, for instance, the case of Trieste tide-gauge, which is affected by the $M_w = 6.5$ Friuli earthquake occurred on May 6, 1976, which is not reported by the PS catalogue but gives a large, mostly postseismic, contribution to the time-histories computed with the CMT.

3.3. Synthetic analysis

All the results presented above show a preferentially positive global trend for seismically induced sealevel variations. In our previous investigations [*Melini et al.*, 2004] we speculated that this behavior might be a consequence of the well-known tendency of seismic energy release to reduce the oblateness of the Earth [*Chao and Gross*, 1987; *Chao et al.*, 1996; *Alfonsi and Spada*, 1998]; nevertheless, this aspect awaits for a better understanding. To this aim, we performed some further analyses.

In figure 9 we plotted the time evolution of relative sealevel variation induced by a point thrust fault with 20° dip angle, seismic moment $M_0 = 10^{21}$Nm at a depth of 20 km. The

RSL variation induced by the fault exhibits well separated lobes of positive and negative variations, whose dimensions are slowly varying with time. Near the epicenter we find an inner zone of negative variation and an outer zone of positive variation that expands with time.

Now we focus our attention on the 1960 Chile earthquake (figure 10) that we know to give a major contribution to the total RSL signal (see also *Melini et al.* [2004]). If we plot the difference $G(t) - u_z(t)$ on both the oceanic and solid surfaces, we can see that the resulting field exhibits a balanced distribution of areas with positive and negative variations, similar to the one shown in figure 9. The orientation of the Chile fault and the geometric properties of the coastlines are such that the coasts, where the majority of PSMSL tide-gauge stations are located, are in the positive RSL lobes.

If we repeat this analysis for the Alaska 1964 (figure 11) earthquake we obtain a similar pattern. Here, the region with negative variations covers part of the North American eastern coast, but in the cumulative results (figures 2 and 3) these negative variations are shadowed by the much larger positive signal induced by the Chile event in the same area.

Therefore we can see that, in assessing the preferentially positive RSL trend predicted by our simulations, a major role is played by the reciprocal geometrical properties of the distribution of tide-gauge stations and orientation of the fault planes of giant earthquakes.

3.4. Effect of the Sumatra-Andaman earthquake

On December 26, 2004 an $M_w = 9.3$ earthquake stroke the northwestern coast of the Sumatra island. Current estimates suggest that this is the second greatest event ever registered. Even if it lies outside the time window of our analysis, we report some preliminary computation about its impact on sealevel.

In figure 12, we show the expected relative sealevel variation following the principal event. The relative sealevel variation remains appreciable over an extremely large area and should give a strong signal on the PSMSL tide-gauge stations located in the region.

For this computation, we modeled the seismic source using a preliminary rupture model (http://www.gps.caltech.edu/ jichen/Earthquake/2004/aceh/aceh.html), which assumes a 450km by 180km rupture plane with 320 degrees strike and 11 degrees dip angles.

Incidentally, we note that for this single event we were able to overcome the point dislocation approximation and to adopt a realistic, finite seismic source. As a consequence we obtained a precise estimate of the geoid correction needed to account for water volume conservation and we ascertained that, as the source refinement increases, the geoid correction tends to decrease.

4. Conclusions

In this work we further analyzed the effect of seismic activity on sealevel variations. We improved our computational methods, enabling us to evaluate the effect of a larger catalogue of earthquakes (as the CMT) on large grids covering the whole oceanic surfaces and to take into account the effects associated with the conservation of the total water volume.

Our results confirm the finding of a previous analysis that, on a global scale, most of the signal is associated with few giant thrust events. These events can induce a sealevel signal on the PSMSL tide gauge stations distributed worldwide of about 0.25 mm/yr. This value is reduced by more than an order of magnitude if the effects of the giant thrust earthquakes of the last century are not considered (i.e. adopting CMT catalog). Since sealevel rise rates associated with climatological factors (water volume increase due to ocean warming

and mass increase from ice melting) are estimated to be at most $1 \div 1.5$ mm/yr [*Levitus et al.*, 2000; *Miller and Douglas*, 2004], the average contribution to RSL coming from seismic activity is not negligible with respect to the climatological factors. Moreover, in regions with strong seismotectonical activity, the seismic contribution amounts up to several mm/yr representing a major contribution to RSL.

In our previous analysis we found that seismicity has an overall tendency to produce a positive RSL variation, but the reason of this behavior was left unexplained. Now, we mostly answered to that question: we found that the RSL field induced by earthquakes has alternating patterns of positive and negative trends, but the geometry of coastlines, where tidal measurements are taken, is such that the majority of tide-gauge stations are located in zones with positive seismic RSL trends.

A question to be faced in future developments will be the role played by tectonical aseismic processes. While our analysis is far from definitely assessing the role of seismic processes in RSL changes, it suggests that the whole tectonic process could be a major non-climatic source of geoid perturbations and RSL variations; controversial evidence come from the results of TOPEX/Poseidon mission that show large deviations from the mean sealevel trend in regions with important tectonic activity. Altough recent investigations have interpreted that satellite-derived sea level trend maps purely in term of thermal expansion [*Willis et al.*, 2004], we think that to obtain a complete understanding of sealevel variations, the seismotectonical contributions can no longer be neglected.

Acknowledgments. We thank the Associate Editor (Ctirad Matyska) and two anonymous reviewers for their incisive comments and helpful suggestions. Partly supported by a MIUR-FIRB research grant.

References

Alfonsi, L., and G. Spada (1998), Effect of subductions and trends in seismically induced earth rotational variations, *J. Geophys. Res.*, *103*(B4), 7351–7362, doi: 10.1029/98JB00079.

Boschi, L., A. Piersanti, and G. Spada (2000), Global postseismic deformation: Deep earthquakes, *J. Geophys. Res.*, *105*(1), 631–652, doi:10.1029/1999JB900278.

Cadek, O., and L. Fleitout (2003), Effect of lateral viscosity variations in the top 300 km on the geoid and dynamic topography, *Geophys. J. Int.*, *152*(3), 566–580, doi: 10.1046/j.1365-246X.2003.01859.x.

Casarotti, E., A. Piersanti, F. Lucente, and E. Boschi (2001), Global postseismic stress diffusion and fault interaction at long distances, *Earth Plan. Sci. Lett.*, *191*(1–2), 75–84.

Cazenave, A., and R. Nerem (2004), Present-day sea level change: observations and causes, *Rev. Geophys.*, *42*, RG3001, doi:10.1029/2003RG000139.

Chao, B., and R. Gross (1987), Changes in the earth's rotation and low-degree gravitational field induced by earthquakes, *Geophys. J. Int.*, *91*(3), 569–596.

Chao, B., R. Gross, and Y. Han (1996), Seismic excitation of polar motion, 1977–1993, *Pure Appl. Geophys.*, *146*, 407–419.

Douglas, B. (1991), Global sea level rise, *J. Geophys. Res.*, *96*(4), 6981–6992, doi: 10.1029/91JC00064.

Douglas, B. (1997), Global sea level rise: a redetermination, *Surv. Geophys.*, *18*(2), 279–292, doi:10.1023/A:1006544227856.

Douglas, B., M. S. Kearney, and S. Leatherman (Eds.) (2001), *Sea Level Rise, History and Consequences*, Academic, San Diego, Calif.

Dziewonski, A., T. Chou, and J. Woodhouse (1981), Determination of earthquake source parameters from waveform data for studies of global and regional seismicity, *J. Geophys. Res.*, *86*(4), 2825–2852.

Levitus, S., J. Antonov, T. Boyer, and C. Stephens (2000), Warming of the World Ocean, *Science*, *287*(5461), 2225–2229, doi:10.1126/science.287.5461.2225.

Marzocchi, W., E. Casarotti, and A. Piersanti (2002), Modeling the stress variations induced by great earthquakes on the largest volcanic eruptions of the 20th century, *J. Geophys. Res.*, *107*(11), 2320, doi:10.1029/2001JB001391.

Melini, D., A. Piersanti, G. Spada, G. Soldati, E. Casarotti, and E. Boschi (2004), Earthquakes and relative sealevel changes, *Geophys. Res. Lett.*, *31*(9), L09,601, doi: 10.1029/2003GL019347.

Miller, L., and B. Douglas (2004), Mass and volume contributions to twentieth century global sea level rise, *Nature*, *428*, 406–409, doi:10.1038/nature02309.

Mitrovica, J., and J. Davis (1995), Present-day post-glacial sea level change far from the late pleistocene ice sheets; implications for recent analyses of tide gauge records, *Bull. Seismol. Soc. Am.*, *22*(18), 2529–2532, doi:10.1029/95GL0224.

Nerem, R. (1995), Global mean sea level variations from topex/poseidon altimeter data, *Science*, *268*, 708–710.

Nerem, R. (1997), Global mean sea level change: correction, *Science*, *275*(5303), 1049–1053, doi:10.1126/science.275.5303.1049i.

Nerem, R., and G. Mitchum (2002), Estimates of vertical crustal motion derived from differences of topex/poseidon and tide gauge sea level measurements, *Geophys. Res. Lett.*, *29*(19), 1934, doi:10.1029/2002GL015037.

Nostro, C., A. Piersanti, and M. Cocco (2001), Normal fault interaction caused by coseismic and postseismic stress changes, *J. Geophys. Res.*, *106*(B9), 19,931–19,410, doi: 10.1029/2001JB000426.

Pacheco, J., and L. Sykes (1992), Seismic moment catalog of large shallow earthquakes, 1900 to 1989, *Bull. Seismol. Soc. Am.*, *82*, 1306–1349.

Peltier, W. (1998), Postglacial variations in the level of the sea: implications for climate dynamics and solid-earth geophysics, *Rev. Geophys.*, *36*(4), 603–689, doi: 10.1029/98RG02638.

Piersanti, A., G. Spada, R. Sabadini, and M. Bonafede (1995), Global postseismic deformation, *Geophys. J. Int.*, *120*(3), 544–566.

Piersanti, A., G. Spada, and R. Sabadini (1997), Global postseismic rebound of a viscoelastic earth; theory for finite faults and application to the 1964 alaska earthquake, *J. Geophys. Res.*, *102*(B1), 477–492, doi:10.1029/96JB01909.

Soldati, G., A. Piersanti, and E. Boschi (1998), Global postseismic gravity changes of a viscoelastic earth, *J. Geophys. Res.*, *103*(12), 29,867–29,886, doi:10.1029/98JB02793.

White, N., J. Church, and J. Gregory (2005), Coastal and global averaged sea level rise for 1950 to 2000, *Geophys. Res. Lett.*, *32*, L01,601, doi:10.1029/2004GL021391.

Willis, J., D. Roemmich, and B. Cornuelle (2004), Interannual variability in upper ocean heat content, temperature, and thermosteric expansion on global scales, *J. Geophys. Res.*, *109*(12), C12,036, doi:10.1029/2003JC002260.

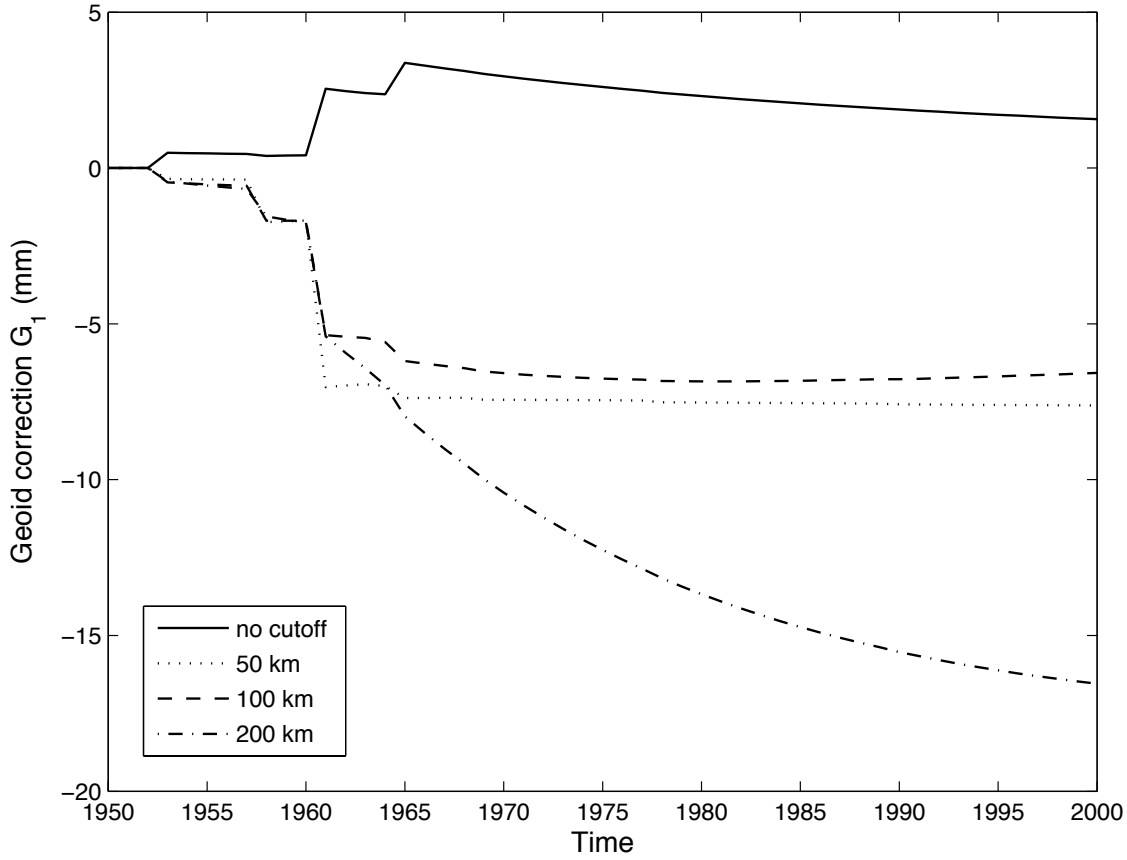

Figure 1. Time-dependent geoid correction that accounts for global water volume conservation. This correction has been computed using 8 earthquakes selected between the largest ones occurred during the last century in the Pacific area. The 4 different curves are computed excluding the integration points located within 4 different cutoff values from the seismic sources (cutoff values are 0, 50, 100 and 200km).

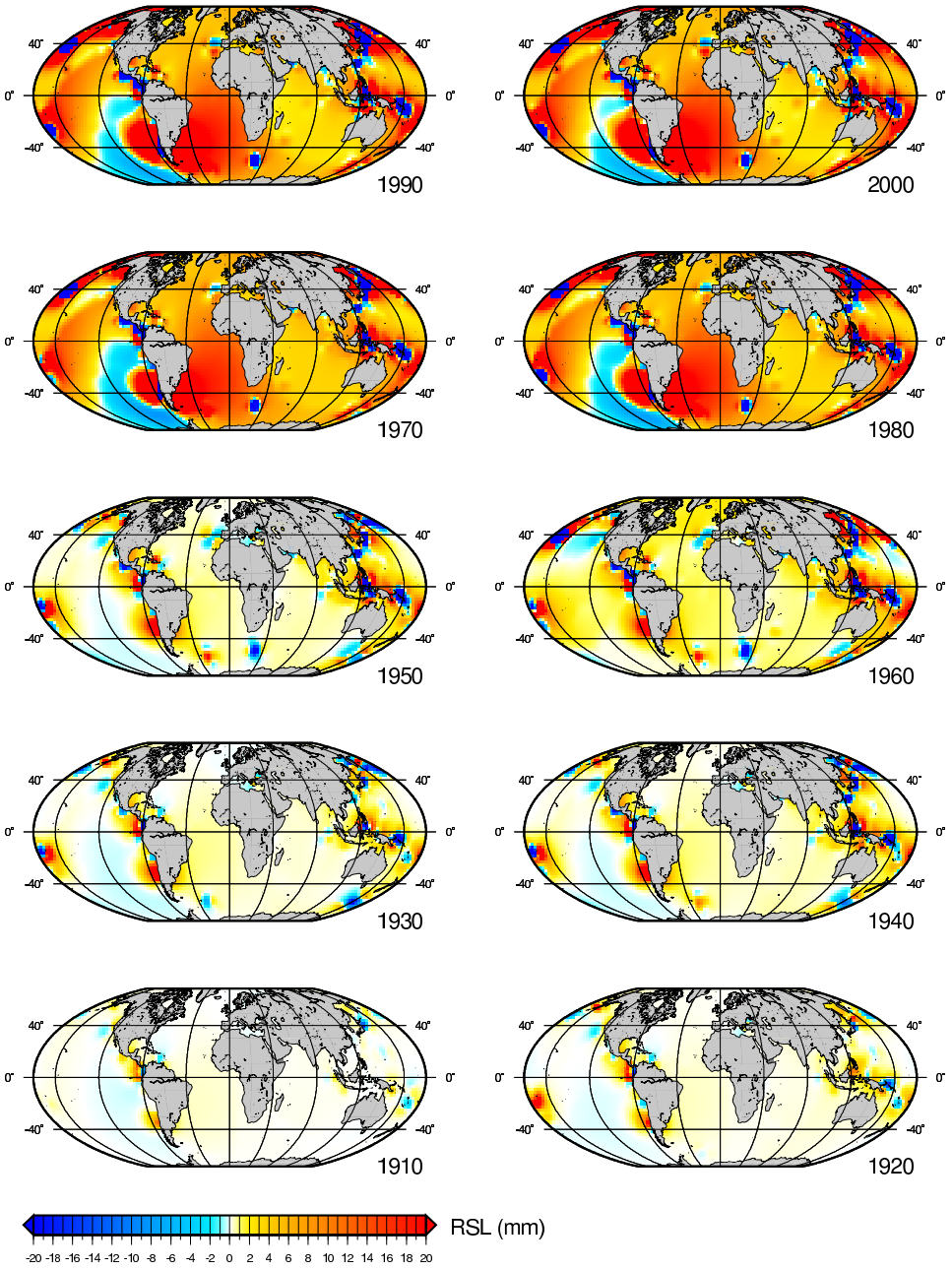

Figure 2. Magnitude of relative sealevel variation over the oceans computed at 10 different times resulting from PS seismic activity. Each map includes the effect of all the earthquakes occurred since the beginning of the catalogue.

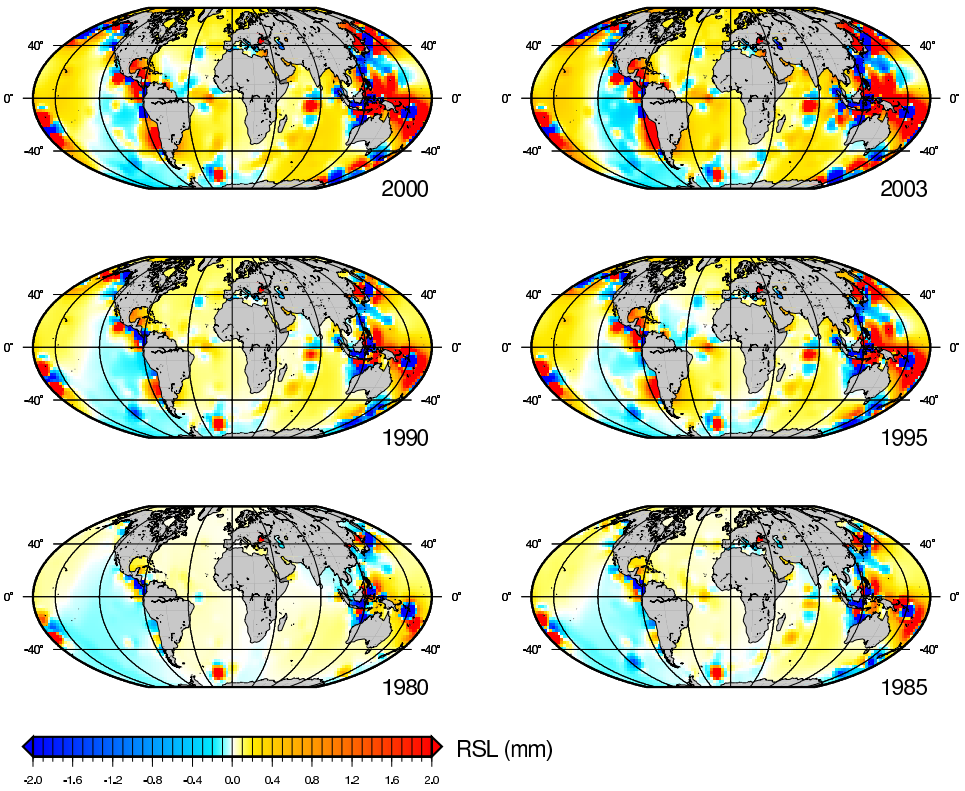

Figure 3. Magnitude of relative sealevel variation over the oceans computed at 6 different times resulting from CMT seismic activity. Each map includes the effect of all the earthquakes occurred since the beginning of the catalogue.

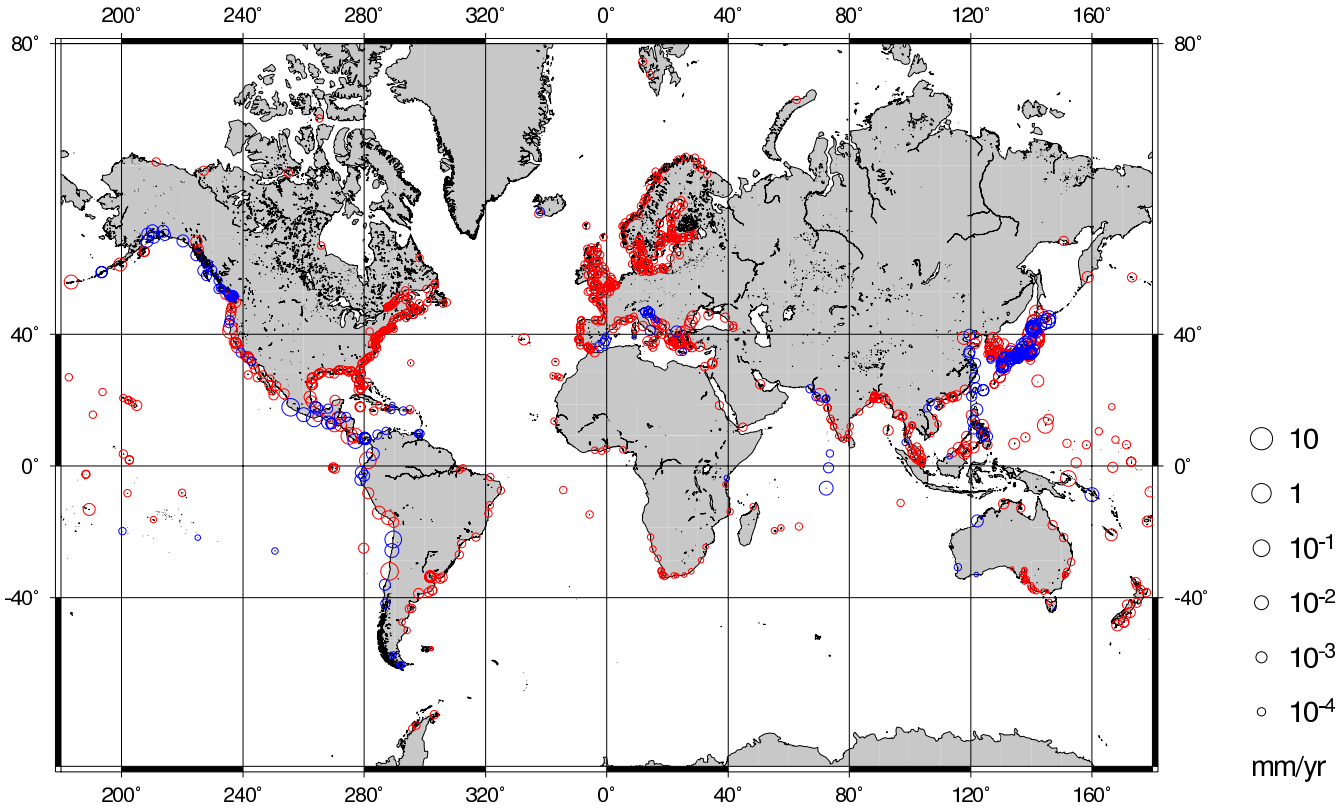

Figure 4. Relative sealevel variation rates over 1976–2003 at the locations of PSMSL tide-gauge stations, resulting from the cumulative effect of CMT seismicity. Red and blue circles correspond to positive and negative trends, respectively.

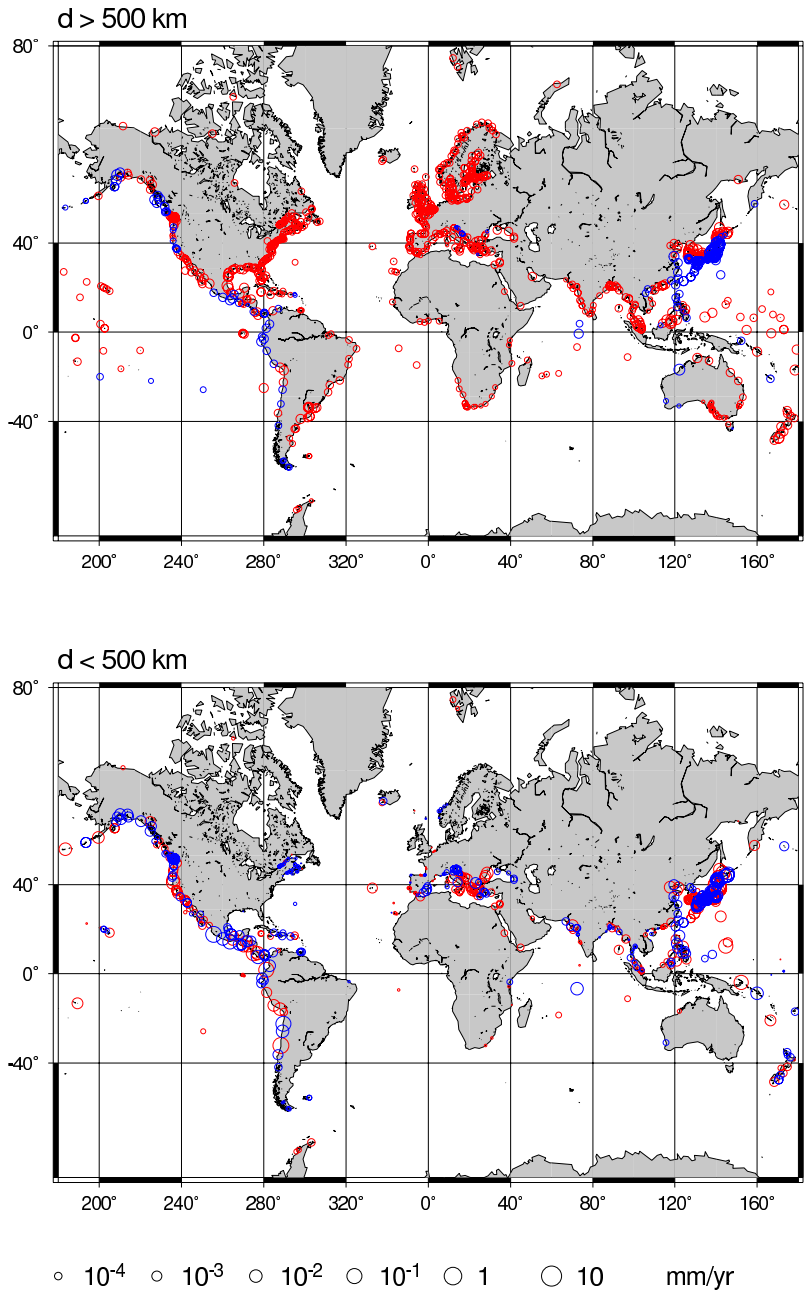

Figure 5. Relative sealevel variation rates over 1976–2003 at the locations of PSMSL tide-gauge stations, resulting from the cumulative effect of CMT seismicity. In the lower panel it is shown only the contribution of earthquakes located within 500 km from each tide-gauge, while in the upper panel it is shown the contribution of earthquakes located at over 500 km from the tide-gauge. Red and blue circles correspond to positive and negative trends, respectively.

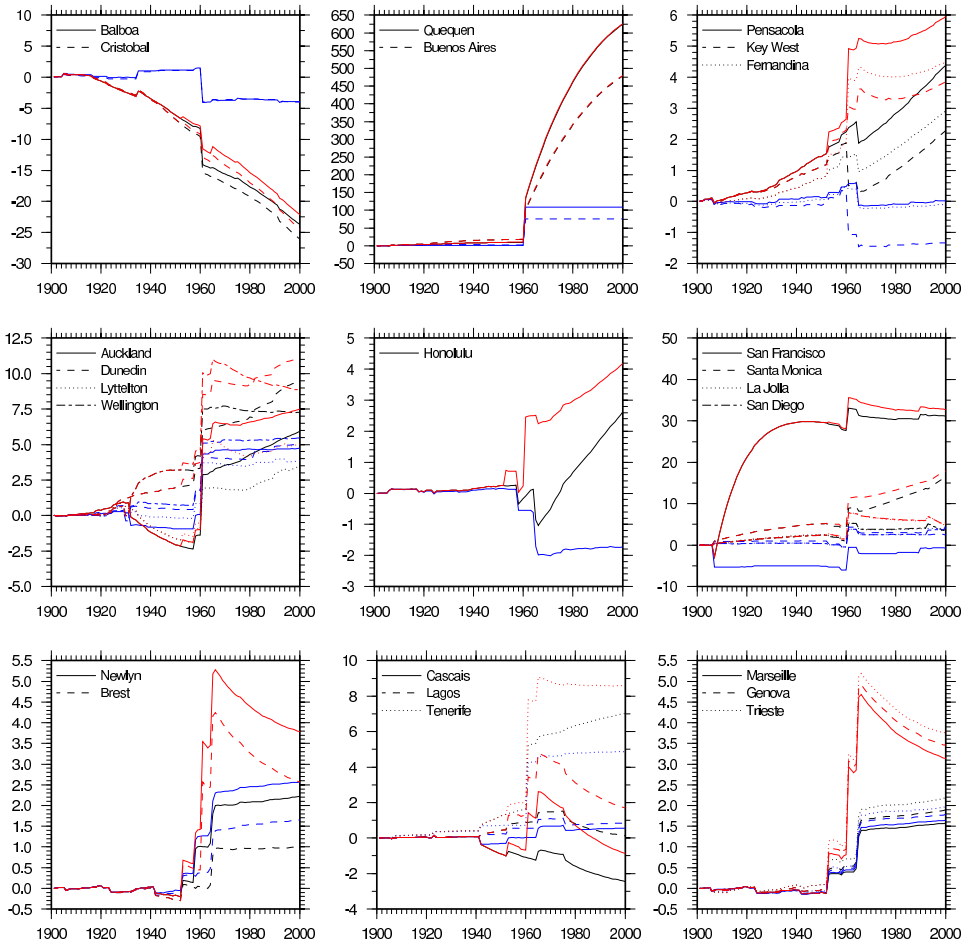

Figure 6. Relative sealevel variation time-histories resulting from PS seismicity on the the tide-gauge sites considered by *Douglas* [1997]. Black and blue lines represent the viscoelastic and purely elastic responses, without taking into account the water volume conservation. Red lines represent the viscoelastic response with water volume conservation.

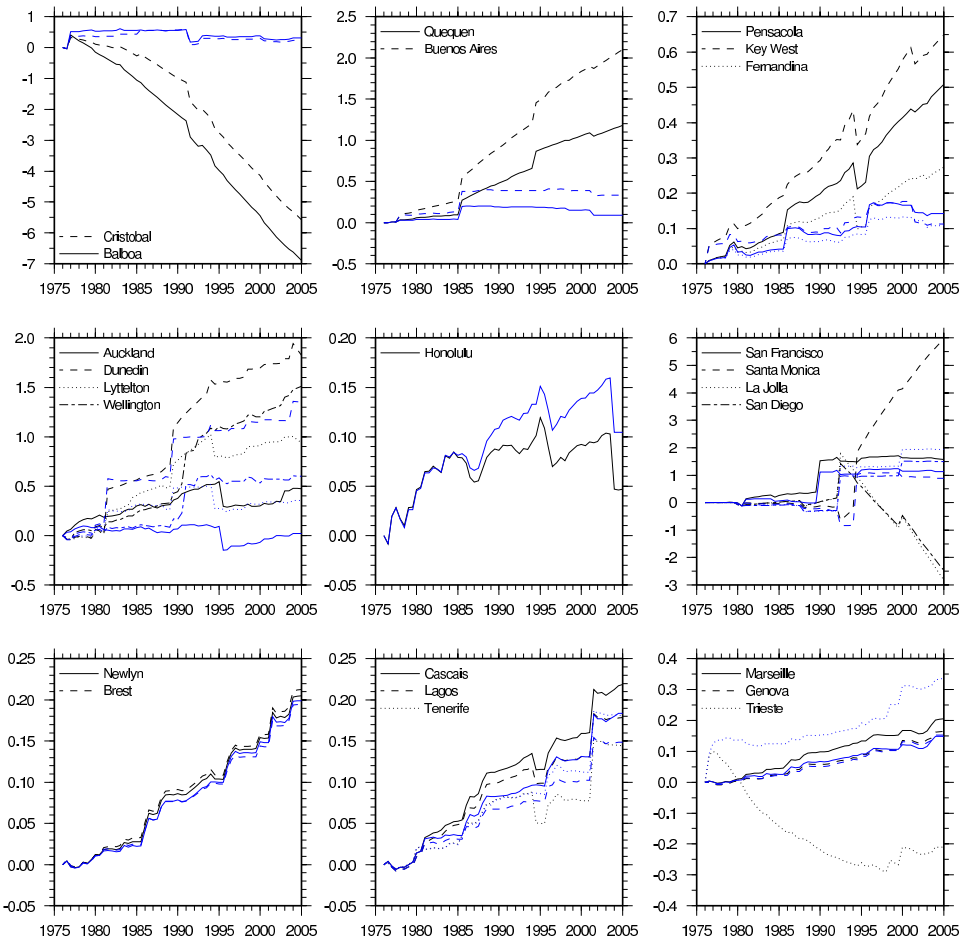

Figure 7. Relative sealevel variation time-histories resulting from CMT seismicity on the tide-gauge sites considered by *Douglas* [1997]. Black and blue lines represent the viscoelastic and purely elastic responses, respectively.

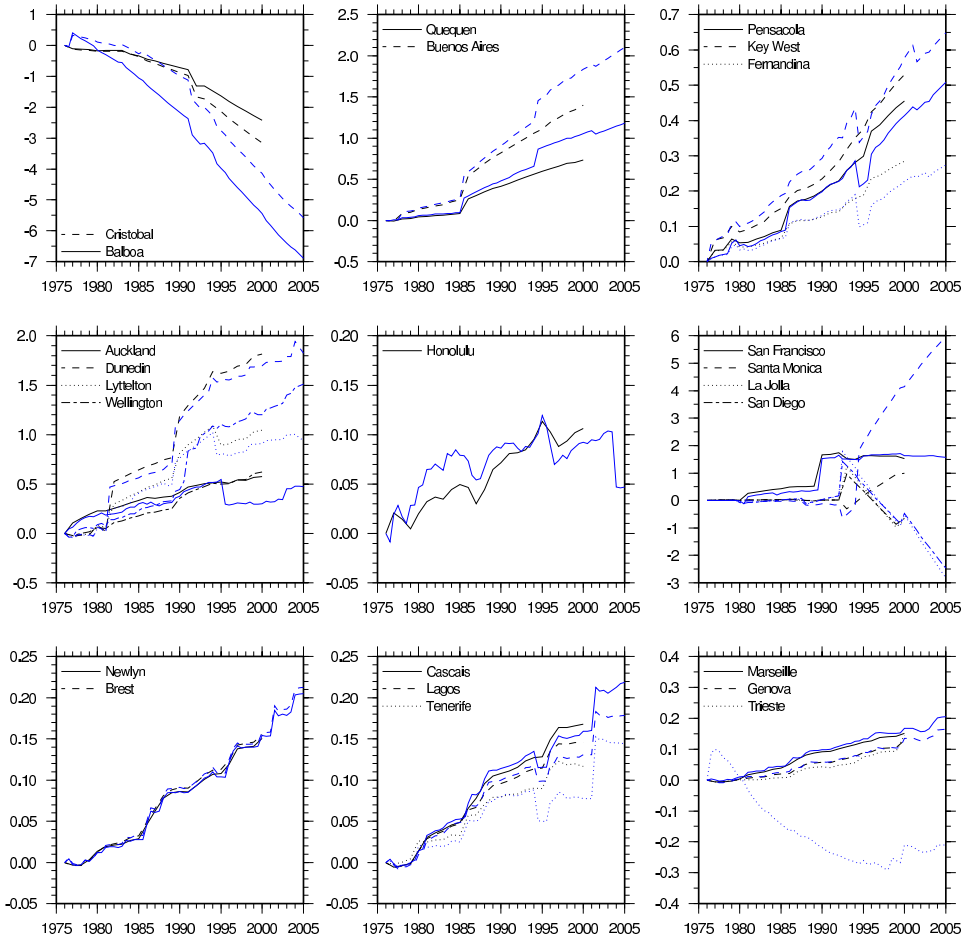

Figure 8. Comparison between the expected seismic RSL signal at the tide-gauge stations considered by *Douglas* [1997] computed using the CMT and PS catalogues in the time-window where the two datasets overlap (1976–2000). Black lines represent the effect of PS seismicity, blue lines the effect of CMT seismicity.

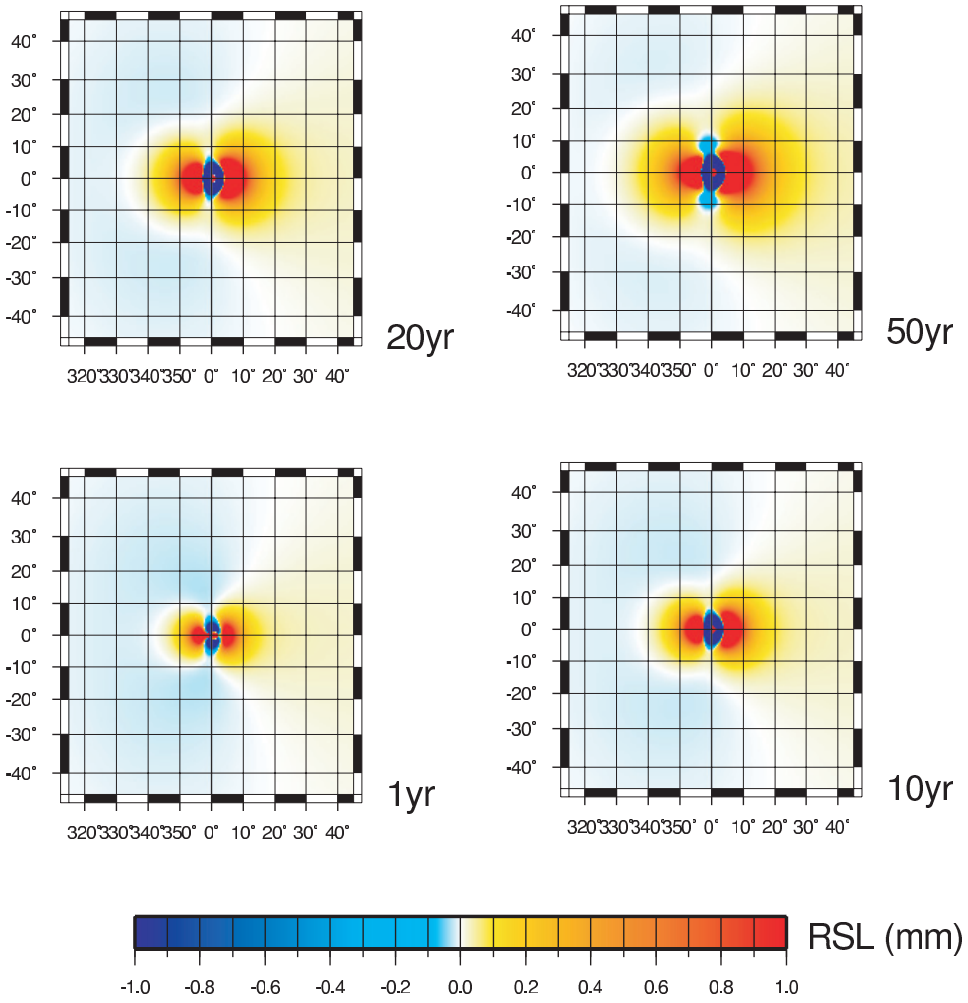

Figure 9. Time evolution of the RSL variation induced by a 20 km deep point thrust fault, with strike along the North direction, dip angle of 20° and seismic moment $M_0 = 10^{21}$ Nm.

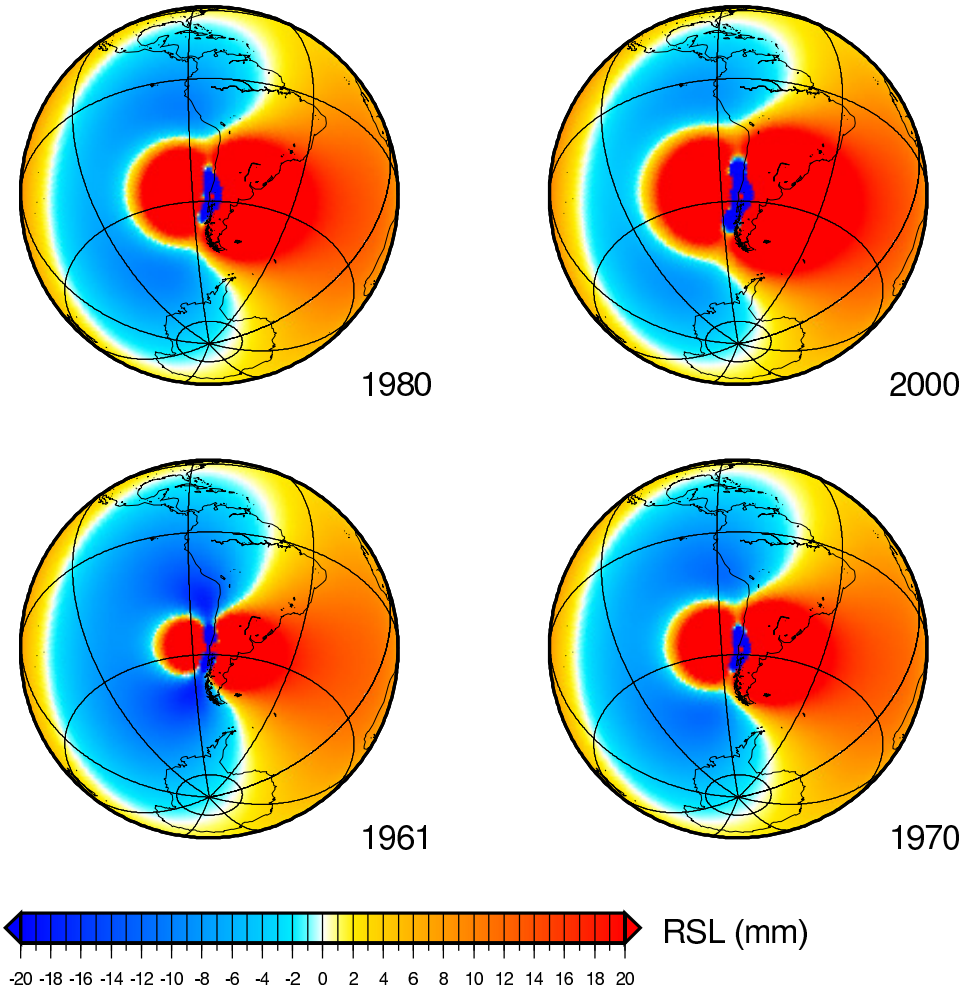

Figure 10. Time evolution of $G(t) - u_z(t)$ associated with the 1960 Chile earthquake. The difference $G - u_z$, when calculated on the oceanic surface, represents the relative sealevel change.

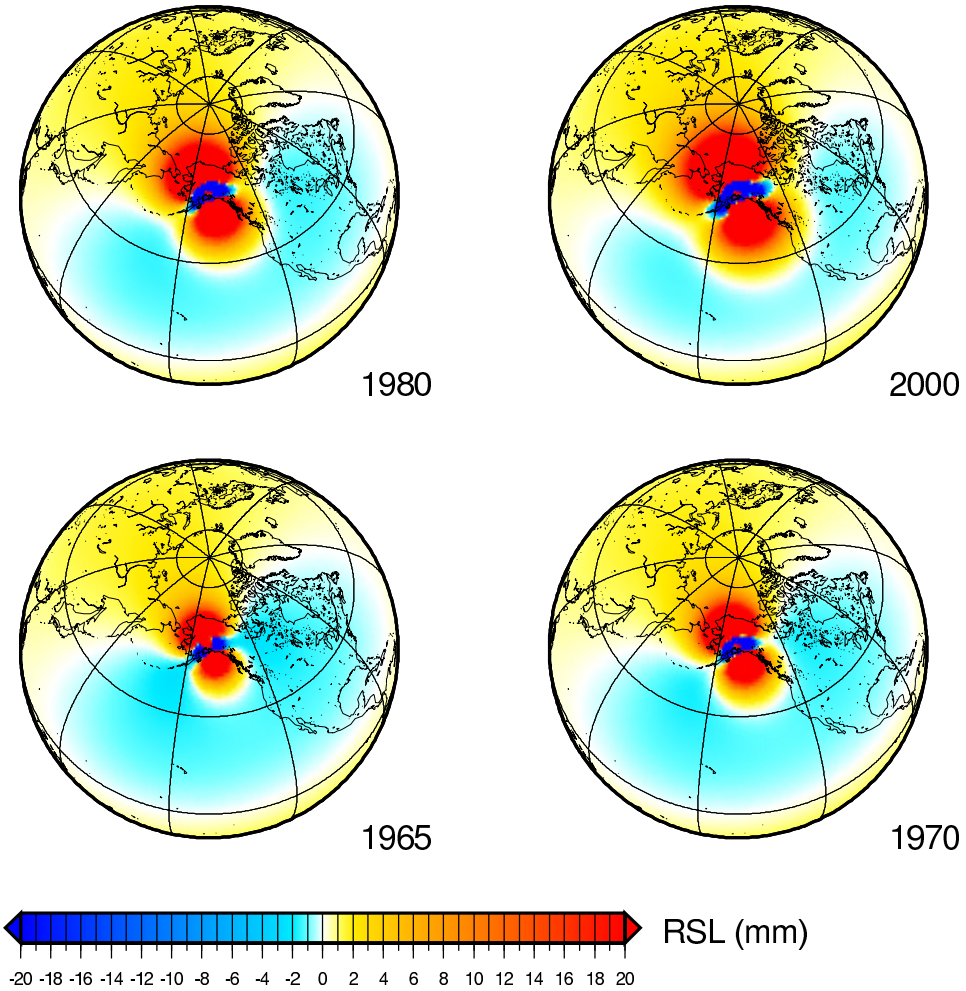

Figure 11. Time evolution of $G(t) - u_z(t)$ associated with the 1964 Alaska earthquake. The difference $G - u_z$, when calculated on the oceanic surface, represents the relative sealevel change.

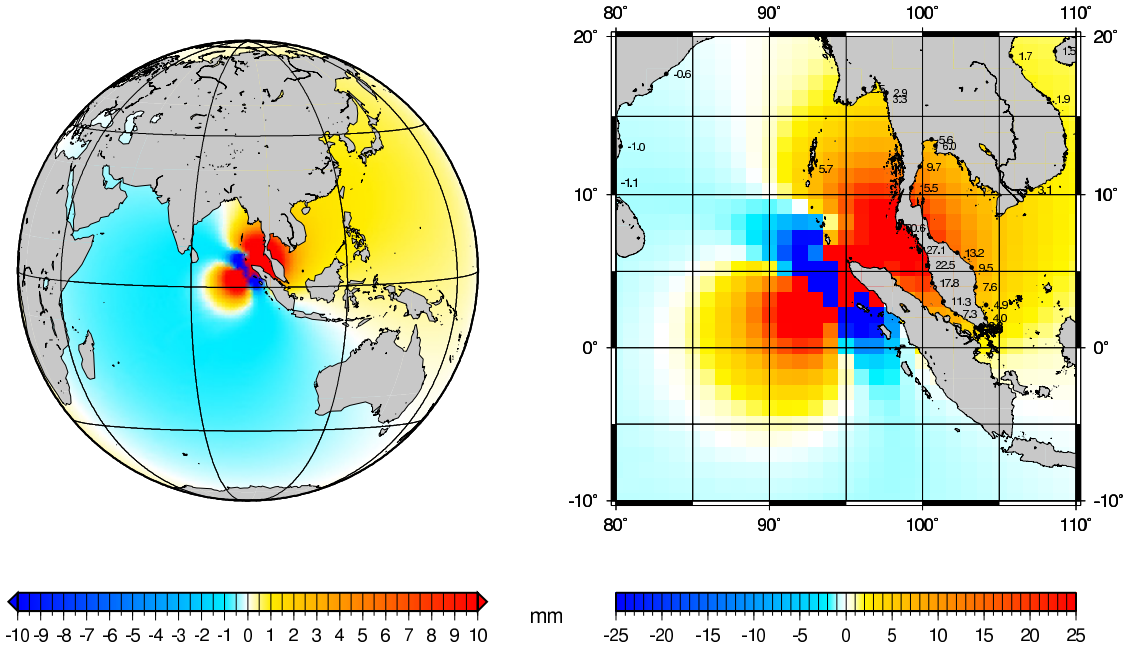

Figure 12. Relative sealevel variation associated with the cosesimic (elastic) deformation and geoid change following the December 26, 2004 Sumatra-Andaman earthquake. In the right panel are reported the locations of PSMSL tide-gauge stations with the predicted coseismic signal (in mm). In the computation of both the RSL field and the coseismic offsets on PSMSL tide-gauges we assumed the conservation of water volume.